- -

Left–Right Multimodal Morphometric Comparison of Human Submandibular Glands

- -

Stimec, Bojan; Ignjatovic, Dejan

How to cite

Communication

Left–Right Multimodal Morphometric Comparison of Human Submandibular Glands

Bojan V. Stimec [1,*] and Dejan Ignjatovic [2,3]

1. Anatomy Sector, Teaching Unit, Faculty of Medicine, University of Geneva, Rue Michel-Servet 1, 1211 Geneva, Switzerland
2. Department of Digestive Surgery, Akershus University Hospital, University of Oslo, 1478 Lorenskog, Norway; dejan.ignjatovic@medisin.uio.no
3. Institute of Clinical Medicine, University of Oslo, 1478 Nordbyhagen, Norway
* Correspondence: bojan.stimec@unige.ch; Tel.: +41-(22)-379-53-20; Fax: +41-(22)-379-52-67

Abstract: This communication study integrates composite multimodal research on postmortem human submandibular glands, based on macromorphometry. The normal ductographic sialograms were pairwise analyzed using linear morphometry, whole-gland planimetry and fractal properties, such as main duct length, caliber and tortuosities, side branches and accessory ducts/lobes. All the examined parameters presented a significant correlation, i.e., symmetry between the left and the right submandibular glands. The morphometric data presented can serve as a valuable reference in clinical practice.

Keywords: submandibular gland; Wharton's duct; anatomy; symmetry; planimetry; postmortem sialography

1. Introduction

The left–right bilateral external symmetry in vertebrates is based on the default symmetric gene expression on the development of mesodermal somites [1,2]). On the other hand, the binary asymmetry involving the internal anatomy of the thorax and abdomen (e.g., greater blood vessels, lungs, heart, digestive tract and its glands) results as a consequence of the switch deviation from the rostro–caudal axis development. The head and neck are also subjects of left–right asymmetries, mainly concerning the muscles, skull and arteries [3–5].

The major salivary glands, being paired, arborized and on the brink between the external and internal morphology, logically pose a question on their laterality. For instance, the submandibular gland, although being smaller than the parotid gland, accounts for two-thirds of the total saliva secretion in quiescent state. This mixed seromucinous tubule–acinar organ consists of a superficial part, which winds around the posterior edge of the mylohyoid muscle and continues as a smaller, deep part; the latter being close to the sublingual gland. The excretory duct of the submandibular gland (Wharton's duct) arises from smaller affluents in the superficial portion and runs through the deep portion, making sharp genu around the said free border of the mylohyoid. Further, after leaving the gland, it courses somewhat upward and forward in the floor of the mouth, between the hyoglossus (medially) and mylohyoid muscle (laterally), and finally opens on the sublingual caruncula, separately or jointly with the major sublingual duct (Bartholin). In the vast majority of cases, the sublingual caruncula are symmetric in position [6].

The asymmetries of the paired head and neck anatomical entities, including the salivary glands, are often ascribed to pathology [7]. For example, the submandibular glands can be affected by a number of processes, such as sialosis, sialolithiasis, autoimmune diseases, sialadenitis, neoplasms, sialoceles and branchial cysts. In Sjögren's syndrome, one of the frequently posed clinical questions is whether there is a horizontal asymmetry, i.e., difference in the left–right severity and spatial involvement [8].

The salivary glands have been analyzed on bases of their flow rates, i.e., their secretory activities, or the influences of age, sex and BMI on their size and fat fraction, as presented on CT and MRI images [9–11]. Both aspects of research should consider the left–right (a)symmetry of the glands.

New mechanistic hypotheses have been proposed on the development of the arborized organs, based on the fingering and branching as a consequence of liquid (or air) being pushed through the output point, with an interface of viscous instability [12]. In this context, one must also wonder whether those physical laws apply symmetrically, or not.

In a comprehensive study on a deep learning model for the delineation and segmentation of head and neck organs at risk for cancer, Zhu et al. [13] produced 3D binary models which, in case of a left and right submandibular gland, presented a high correlation in the test performance.

On the other hand, the unilateral aplasia of the major salivary glands are rare entities, detected as incidental findings on imaging. They can occur separately, or in conjunction with the hypertrophy of the contralateral gland, or other ipsilateral major glands [14,15].

The common quotient of all the mentioned studies is the question about whether there is a difference in the macromorphology of the normal left and right submandibular gland, as a consequence of anatomical variability. In order to answer this question, we carried out a composite multimodal morphometric analysis of postmortem submandibular glands, including linear morphometry, planimetry and fractal properties. Therefore, the Results section of the article is subdivided into those three headers.

2. Material and Methods

The research was performed in accordance with the Ethical Principles for Medical Research Involving Human Subjects (World Medical Association, Declaration of Helsinki: Ethical Principles for Medical Research) and legislative points of the Law on Health Protection, including the Chapter on establishing the time and cause of death and on the autopsy of a deceased person and the Chapter on the procurement of bodies of deceased persons for the purpose of practical medical education. The local health legislature allowed research on donated bodies. As the data did not contain personal identifiers (anonymous biological material), this research did not require an IRB review under federal law (Human Research Act 810.30, HRA).

The human postmortem material in this study included fresh samples of head and neck organs, harvested during autopsies, from adults of both sexes from different age groups, but all from the same ethnic background (West Balkans). In the choice of salivary glands, we opted for the submandibular, as the complete excision of the parotid gland leads to face mutilation, and the submandibular gland is more easily accessible. Concerning the histology of the two glands, the lobules are smaller in the parotid gland, but the micromorphology of the periductal connective tissue is analogous [16]. The samples, excised en bloc, consisted of the cervical trachea, larynx, thyroid gland, pharynx (except nasopharynx), hyoid bone, tongue and floor of the mouth with the submandibular and sublingual salivary glands. Special care was taken to preserve the submandibular glands and their ducts intact during the procedure, and the neighboring structures prevented deformation of ducts during manipulation. The cases with macroscopically visible and/or palpable changes, as well as with trauma of the head–neck region were excluded from the study. In all the included cases, the cause of death was not related to the harvested organs and their vicinities.

The linear morphometry study comprised 18 specimens (14 males, 4 females; mean age: 49.9 years), the planimetry study was based on 22 specimens (17 males, 5 females, mean age: 57.9 years), and the fractal properties study included 42 specimens (35 males, 7 females, mean age: 53.1 years).

After shortly being rinsed in running water, a specimen was placed flat on its dorsal surface, and the sublingual caruncle and the Wharton's duct were cannulated using a thin Venflon catheter. An 80% suspension of barium sulphate, diluted in formaldehyde, was

carefully injected under controlled pressure, until there was resistance felt, or there was an appearance of contrast in the small ducts on the gland surface. The barium contrast was used instead of iodine contrast for better opacification of the ductal system, as the latter tends to rapidly enter the acini and blur the image with parenchymography. Likewise, the barium sulphate was diluted in order to be less viscous.

Immediately after injection, the specimens underwent image acquisition on standard radiographic equipment. Their positions in the frontal and the axial planes were controlled beforehand and verified via fluoroscopy (Figures 1 and 2). A metal reference lamina of known width was placed in the vicinity of the specimen, for the purpose of the calibration of dimension, i.e., resolving the magnifying influence of distance between the X-ray tube and the specimen (film). Sialograms were taken under the following parameters: a generator of 42–50 kV and exposure of 3.2–5.0 mAs.
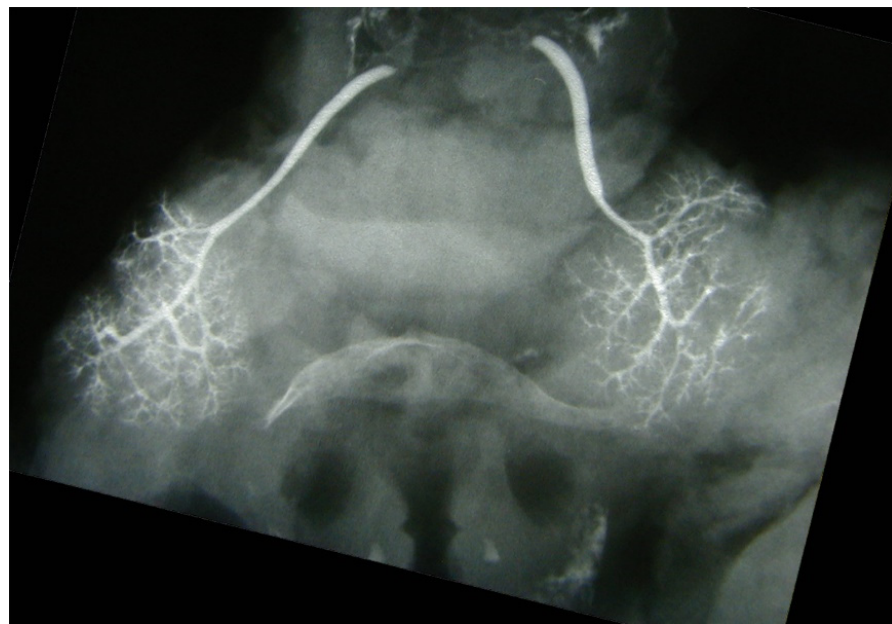
Figure 1. Postmortem sialography of submandibular glands, coronal plane. The ductal arborization is distinct. Hyoid bone is visible in the middle of the image.
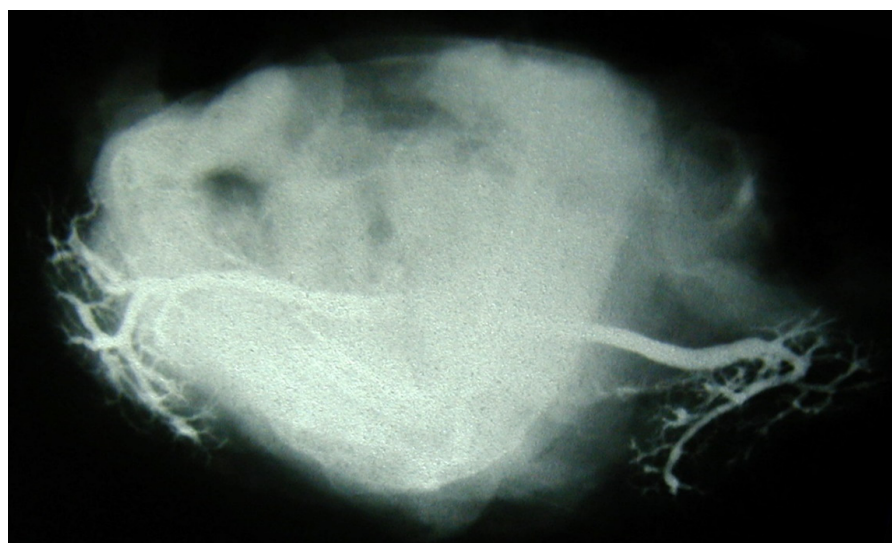
Figure 2. Postmortem sialography of submandibular glands, axial plane. The genu of Wharton's duct is clearly visible.

A preliminary image analysis was used to evaluate the filling of ducts and detect eventual overseen pathology on ductograms. There were three cases with insufficient filling, and another three with a dilated, "amputated" and/or tortuous side and terminal branches of the submandibular duct, as well as with the dilation of the duct itself. These 3 cases underwent tissue sampling, hematoxylin–eosin and Masson's trichrome staining and light microscopy. Histology revealed ductal ectasia, advanced fibrosis and adipose tissue infiltration, which were in correlation with ductography and with clinical evidence of alcohol abuse. These six cases were excluded from the study.

The image analysis of the sialograms was achieved by means of the ImageJ, public domain Java image processing software (ImageJ 1.53e, Research Services Branch, National Institute of Mental Health, Bethesda, MD, USA). First, the scale was calibrated with respect to the known width of the metal reference lamina. The palette of tools used was as follows: straight line for calibers of the duct and diameters of the whole gland, area for the contour outline of the maximal cross-sectioned surface, i.e., planimetry, angle for inclination gradient and freehand line for non-linear lengths.

The data underwent analyses with the software engine Statistica 64-bit v. 13.5.0.17 (TIBCO Software Inc. 2018, Santa Clara, CA, USA), including a Power Analysis, Sample Size Calculation, multivariate analysis of variance, Shapiro–Wilk W test for normality of distribution, Student's *t* test, Pearson's correlation coefficient for continuous variables, and Spearman's rank order correlation, or the Fisher exact test for categorical variables.

3. Results

Linear Morphometry [17]

The first item was the caliber of the submandibular duct, measured at three distinct portions—proximal, middle and distal third, with the mean totals ($\pm$SD) being 1.81 ± 0.63 mm, 1.85 ± 0.54 mm and 1.74 ± 071 mm for the right gland and 1.65 ± 0.52 mm, 1.78 ± 0.61 mm and 1.80 ± 0.51 mm for the left gland, respectively. When comparing the left and the right calibers at the three mentioned sites, there were no statistically significant differences: $p = 0.46$, $p = 0.59$ and $p = 0.19$, respectively. The same result was obtained on evaluating the left–right asymmetry of Wharton's duct length ($p = 0.13$). The genu of the submandibular duct was measured in the axial plane; the average on the right was 121.3 ± 25.9 degrees, 107.5 ± 25.0 degrees, without mutual differences ($p = 0.89$). The approximate gland size was measured in the coronal plane, through a maximal longitudinal (mean: right, 44.6 ± 12.8 mm; left, 43.7 ± 10.1 mm) and maximal transverse (mean: right, 27.0 ± 8.0 mm; left, 24.9 ± 6.2 mm) diameter of the contours of the gland. Again, there were no left-right differences; the *p* values were 0.33 and 0.29 for the longitudinal and transverse diameters, respectively.

Planimetry of sialograms [18]

The mean planimetric sizes of the glands were 872 ± 154 mm^2 (right) and 836 ± 144 mm^2 (left). The first issue was to test the influence of age on the gland size, where a multivariate analysis of variance produced no significance ($p = 0.197$). The next step was to compare right and left glands and, again, there was no statistically significant difference ($p = 0.390$). When testing the sex differences, the submandibular glands, taken together left and right, were larger in males than in females ($p < 0.001$).

Fractal properties [19]

The first item analyzed was the length of Wharton's duct, defined intraglandularly as the largest canal extending from the pole of the gland to the extraglandular portion of the duct. The average total duct lengths were 63.8 ± 10.2 mm and 61.8 ± 8.9 mm for the right and left glands, respectively. The intraglandular portion of the submandibular duct was less than a half of the whole total length (29.4 ± 5.4 mm—right, 28.5 ± 5.8 mm—left). A paired correlation test found no left–right differences, for both items: the total and intraglandular length, $p < 0.001$ and $p = 0.05$, respectively. When assessing the course of Wharton's duct, we noted kinks and tortuosities apart from the regular genu of the duct. They were found

in 32.4% of the right glands, and 23.7% of the left glands. These values, tested using Fisher's exact test, also correlated statistically ($p = 0.279$).

The next object of interest was, logically, the caliber of the submandibular duct. This dimension is difficult to assess, as it changes along the course of the duct [20]. Therefore, we chose the maximal value of the duct as a more comparable reference for each gland. The mean calibers were 2.6 ± 0.5 mm and 2.3 ± 0.5 mm for the right and the left glands, respectively. This morphometric factor presented a highly significant correlation ($p < 0.001$) between the two glands in each subject.

The median total number of intraglandular side branches, i.e., affluents to Wharton's duct was nine (SD = 2.5), both for the right and the left glands. Despite the high variability, this number presented a normal distribution, and again, the correlation between the two sides was highly significant ($p = 0.001$).

The last item analyzed was the existence of accessory submandibular lobes/duct. They were found in 8.1% on the right side only, 5.3% on the left side only and in 5.3% bilaterally.

4. Discussion

The caliber of the submandibular duct is a valuable parameter of the state of the gland, concerning that the duct can undergo cystic dilatations, narrowing and atresia [20]. When comparing the absolute values of the duct with the histology studies [21], it is obvious that our results present higher values. Such a difference can be explained twofold: there is an injection pressure on one side, and a retraction of tissue during fixation, on the other. However, no left–right asymmetries were detected.

It is worth noting that the trajectory of Wharton's duct course is somewhat directed superiorly, thus opposing gravity in the upright position. Also, there is the presence of the genu of Wharton's duct [22], a common site of sialolithic obstruction. As the angle of this duct changes with the point of view, we chose the axial plane as being the most realistic. A high left–right accordance was found for this item, as well.

Finally, the size of the gland was approximated by using the two orthogonal axes, longitudinal and transverse. Apart from pathological processes, the size is affected by congenital involution (with contralateral hypertrophy), and by laterality—e.g., dextral persons have stronger intrinsic and extrinsic masticatory musculature on the right side, which can also affect the submandibular gland [23]. In contrast to this, we found no left–right differences, which is in line with the findings of Heo et al. [10].

The major salivary glands were assessed using a wide range of imaging methods, including conventional sialography, CT, MRI, ultrasound, scintigraphy and contrast MRI sialography [20]. We chose sialography, as it, at the same time, produces the full ductal arborization and provides the contours of the gland for size assessment. In comparison to the linear morphometry, the sizes of the glands can be more precisely assessed through planimetry, as shown by a comprehensive parenchymographic study on pancreases [24], which found a positive correlation between the 2D gland surface and its volume and weight. The same method was applied on salivary glands and revealed a strong ipsilateral correlation between the parotid and the submandibular gland. Therefore, we implemented this method on our series of submandibular sialograms.

Our findings agree with the computerized automatic object recognition model, within the CT and MRI quantitative radiology [25], which underlines symmetry in the sizes of bilateral organs, irrespective of the subject's body size. Also, our results confirm the CT findings on healthy volunteers [10], namely, the maximal cross-sectional area of the submandibular gland is larger in males than in females, and there is correlation between the right and left glands with respect to the same parameter. It is worth noting that this study [10] noted that age affects the CT number of the salivary glands.

Other important issues of the planimetric approach with postmortem sialographic specimens include an accurate manual quantitative analysis, the presentation of the canalicular branching and microscopic assessments of excised samples. This last item can be performed on the living via fine-needle biopsy [26].

Bearing in mind that the submandibular gland curves around the mylohyoid muscle and therefore has a somewhat irregular shape, we chose the maximal cross-section projection of the gland, which lies in the coronal plane. This approach leads to the best ratio between the size of the gland and its planimetric surface.

The submandibular gland most often changes its dimensions due to different pathological processes, such as tumors, alcoholic sialosis or sialadenitis, but there is also a functional etiology—bulimia nervosa [27]. Our three cases excluded for pathology conformed to the history of alcoholism, presenting at histology the adipose tissue infiltration of the stroma, advanced fibrosis, ductal dilatation and interstitial edema.

Last, but not least, the significantly larger submandibular glands in males found in our series are in accord with similar results from CT volumetric studies on the pancreas [28].

Morphometric analyses of human anatomy face obstacles when confronted with entities that do not fall within the scope of Euclidean geometry, because of their irregular forms. Here, another aspect appears—fractal geometry [29]. In short, this entity implies that irregular objects (or organs) have a self-similarity in structure, expressing the analogous non-integer geometric property at different scales. This self-semblance pattern repeats cyclically at several size levels. This morphological complexity has been observed and validated in organs, tissues and cells [30].

Our study made a step forward in relation to the previously mentioned delineation of the submandibular gland [26], presenting the particularities of Wharton's duct: its dimensions, course and ramifications. This detailed approach has its clinical logic, because the chronic sialadenitis of different etiologies comprises several structural levels: the destruction of acini and perilobular and periductal fibrosis [31,32]. Our findings of Wharton's duct dimensions (caliber, length) were a little larger in comparison to the findings of digital subtraction sialography in the literature [31], but this can be ascribed to the differences in the methodological approach, i.e., to the stronger manual contrast injection and absence of muscle tonus in postmortem sialography. Despite these differences, the mutual comparison of glands in each subject revealed a left–right symmetry of Wharton's duct dimensions.

Yet another feature of Wharton's duct plays a significant role in salivary diagnostics and therapy—the course of the duct. The clinical significance of the tortuosities lies in discriminating diseased and healthy organs. Further, kinks of the principal duct can render procedures like balloon dilatation difficult [33]. We have noted tortuosities in one third and one fourth of the right and left submandibular ducts, respectively. This difference did not reach the level of statistical significance; therefore, they can be attributed to anatomical variation.

In cases of chronic pancreatitis, as well as in autoimmune diseases such as Sjogren's, there is a wide palette of pathological changes which affect the primary and secondary peripheral branches of Wharton's duct. For instance, sialography can reveal dilatations (cystic or non-cystic), ductal ectasia, parietal irregularities and a lack of opacification ("amputation") of the ducts [34]. All these changes can imply initial or mild inflammation. On the other hand, it has been noted that conventional or subtraction sialography present more side branches than MR sialography [35]. Our initial sample of sialograms included three cases with such changes, which were confirmed through heteroanamnestic data (alcoholism) and histology. After excluding these three cases (and three more with insufficient injection), the remaining sialograms presented a full arborization of the ducts and were therefore eligible for morphometric analyses. Both the left and the right submandibular glands presented a median of nine primary side branches; hence, this item has also been symmetrical.

The final portion of this study was the identification of accessory lobes and/or ducts. If found in the downstream portion of Wharton's duct, they can most probably be attributed to a greater sublingual gland [36]; however, in our case, they were in close proximity to the submandibular gland. We did not include such separate, independent glands [37]; we rather opted for the budding of the principal gland. A small number of these outgrowths were found, both on the left and on the right sides and bilaterally.

5. Conclusions

Our comprehensive study has provided detailed morphometry of the normal submandibular glands and their ducts through different means of analyses—linear, planimetric and fractal. In regard to all the parameters assessed, the left–right comparison revealed the full symmetry of this paired organ. Further, these data can serve as a reference point for clinical diagnostics.

References

1. MacLean, K.; Dunwoodie, S.L. Breaking symmetry: A clinical review of left-right patterning. *Clin. Genet.* **2004**, *65*, 441–457. [CrossRef] [PubMed]
2. Burwell, R.G.; Dangerfield, P.H.; Freeman, B.J.C.; Aujla, R.K.; Cole, A.A.; Kirby, A.S.; Pratt, R.K.; Webb, J.K.; Moulton, A. Etiologic theories of idiopathic scoliosis: The breaking of bilateral symmetry in relation to left-right asymmetry of internal organs, right thoracic adolescent idiopathic scoliosis (AIS) and vertebrate evolution. *Stud. Health Technol. Inform.* **2006**, *123*, 385–390. [PubMed]
3. Toni, R.; Casa, C.D.; Castorina, S.; Roti, E.; Ceda, G.; Valenti, G. A meta-analysis of superior thyroid artery variations in different human groups and their clinical implications. *Ann. Anat.* **2004**, *186*, 255–262. [CrossRef] [PubMed]
4. Hayashi, Y.; Tachiki, C.; Morikawa, T.; Aihara, Y.; Matsunaga, S.; Sugahara, K.; Watanabe, A.; Kawamata, T.; Nishii, Y. Three-Dimensional Analysis of the Cranial Base Structure in Patients with Facial Asymmetry. *Diagnostics* **2023**, *14*, 24. [CrossRef] [PubMed]
5. Naghdi, N.; Elliott, J.M.; Weber, M.H.; Fehlings, M.G.; Fortin, M. Cervical muscle morphometry and composition demonstrate prognostic value in degenerative cervical myelopathy outcomes. *Front. Neurol.* **2023**, *14*, 1209475. [CrossRef] [PubMed]
6. Abba, M.; Abramson, A.; Tunis, T.S.; Roitblat, Y.; Shilco, P.; Vaiman, M. The Normative Topographic Position of the Wharton's Duct Orifice in Adults. *J. Oral Maxillofac. Surg.* **2022**, *80*, 913–919. [CrossRef] [PubMed]
7. Welkoborsky, H.J.; Jecker, P. (Eds.) *Ultrasonography of the Head and Neck. An Imaging Atlas*, 1st ed.; Springer: Cham, Switzerland, 2019; pp. 15–39, 235–257.
8. Golder, W.; Stiller, M. Distribution pattern of Sjögren's syndrome: A sialographical study. *Z. Rheumatol.* **2014**, *73*, 928–933. [CrossRef] [PubMed]
9. Wang, Z.; Shen, M.-M.; Liu, X.-J.; Si, Y.; Yu, G.-Y. Characteristics of the saliva flow rates of minor salivary glands in healthy people. *Arch. Oral Biol.* **2015**, *60*, 385–390. [CrossRef]
10. Heo, M.S.; Lee, S.C.; Lee, S.S.; Choi, H.M.; Choi, S.C.; Park, T.W. Quantitative analysis of normal major salivary glands using computed tomography. *Oral Surg. Oral Med. Oral Pathol. Radiol. Endod.* **2001**, *92*, 240–244. [CrossRef]
11. Su, G.Y.; Wang, C.B.; Hu, H.; Liu, J.; Ding, H.Y.; Xu, X.Q.; Wu, F.Y. Effect of laterality, gender, age and body mass index on the fat fraction of salivary glands in healthy volunteers: Assessed using iterative decomposition of water and fat with echo asymmetry and least-squares estimation method. *Dentomaxillofac. Radiol.* **2019**, *48*, 20180263. [CrossRef]
12. Fleury, V. Sur une symétrie fondamentale entre la morphogenèse et le fonctionnement des organes arborisés. *CR Acad. Sci. Paris Life Sci.* **2001**, *324*, 405–412. [CrossRef]

13. Zhu, W.; Huang, Y.; Zeng, L.; Chen, X.; Liu, Y.; Qian, Z.; Du, N.; Fan, W.; Xie, X. AnatomyNet: Deep learning for fast and fully automated whole-volume segmentation of head and neck anatomy. *Med. Phys.* **2019**, *46*, 576–589. [CrossRef]
14. Kandemirli, S.G. Unilateral Submandibular Gland Aplasia Mimicking Nodal Metastasis. *J. Pediatr. Hematol. Oncol.* **2020**, *42*, 220–221. [CrossRef]
15. Cilingiroglu Anli, S.; Kazak, Z. Bilateral variation of the parotid gland in cadaver: A case report. *Nagoya J. Med. Sci.* **2023**, *85*, 388–394.
16. Hosoyamada, Y.; Sakai, T. The ultrastructure of periductal connective tissue and distinctive populations of collagen fibrils associated with ductal epithelia of exocrine glands. *Arch. Histol. Cytol.* **2003**, *66*, 407–418. [CrossRef] [PubMed]
17. Stimec, B.; Nikolic, S.; Rakocevic, Z.; Bulajic, M. Symmetry of the submandibular glands in humans—A postmortem study assessing the linear morphometric parameters. *Oral Surg. Oral Med. Oral Pathol. Oral Radiol. Endod.* **2006**, *102*, 391–394. [CrossRef] [PubMed]
18. Stimec, B.V.; Rakocevic, Z.; Ignjatovic, D.; Fasel, J.H.D. Planimetric correlation between the submandibular glands and the pancreas: A postmortem ductographic study. *Anat. Sci. Int.* **2018**, *93*, 114–118. [CrossRef]
19. Stimec, B.V.; Ignjatovic, D.; Lobrinus, J.A. Establishing correlations between normal pancreatic and submandibular gland ducts. *BMC Gastroenterol.* **2022**, *22*, 362. [CrossRef] [PubMed]
20. Morimoto, Y.; Tanaka, T.; Yoshioka, I.; Masumi, S.; Yamashita, M.; Ohba, T. Virtual endoscopic view of salivary gland ducts using MR sialography data from three dimension fast asymmetric spin-echo (3D- FASE) sequences: A preliminary study. *Oral. Dis.* **2002**, *8*, 268–274. [CrossRef]
21. Zenk, J.; Hosemann, W.G.; Iro, H. Diameters of the main excretory ducts of the adult human submandibular and parotid gland: A histologic study. *Oral Surg. Oral Med. Oral Pathol. Oral Radiol. Endod.* **1998**, *85*, 576–580. [CrossRef] [PubMed]
22. Drage, N.A.; Wilson, R.F.; McGurk, M. The genu of the submandibular duct—Is the angle significant in salivary gland disease? *Dentomaxillofac. Radiol.* **2002**, *31*, 15–18. [CrossRef]
23. Korotko, G.F.; Kadirov, S.H. The bilateral autonomy of enzyme secretion by human salivary glands. *Stomatologiia* **1994**, *73*, 26–28.
24. Stolte, M. *Chronische Pankreatitis*; Perimed Fachbuch-Verlagsgesellschaft: Erlangen, Germany, 1984; pp. 21–31.
25. Udupa, J.K.; Odhner, D.; Zhao, L.; Tong, Y.; Matsumoto, M.M.; Ciesielski, K.C.; Falcao, A.X.; Vaideeswaran, P.; Ciesielski, V.; Saboury, B.; et al. Body-wide hierarchical fuzzy modeling, recognition, and delineation of anatomy in medical images. *Med. Image Anal.* **2014**, *18*, 752–771. [CrossRef]
26. Cohen, E.G.; Patel, S.G.; Lin, O.; Boyle, J.O.; Kraus, D.H.; Singh, B.; Wong, R.J.; Shah, J.P.; Shaha, A.R. Fine-Needle Aspiration Biopsy of Salivary Gland Lesions in a Selected Patient Population. *Arch. Otolaryngol. Head Neck Surg.* **2004**, *130*, 773–778. [CrossRef] [PubMed]
27. Metzger, E.D.; Levine, J.M.; McArdle, C.R.; Wolfe, B.E.; Jimerson, D.C. Salivary gland enlargement and elevated serum amylase in bulimia nervosa. *Biol. Psychiatry* **1999**, *45*, 1520–1522. [CrossRef] [PubMed]
28. Djuric-Stefanovic, A.; Masulovic, D.; Kostic, J.; Randjic, K.; Saranovic, D. CT volumetry of normal pancreas: Correlation with the pancreatic diameters measurable by the cross-sectional imaging, and relationship with the gender, age, and body constitution. *Surg. Radiol. Anat.* **2012**, *34*, 811–817. [CrossRef] [PubMed]
29. Grizzi, F.; Spadaccini, M.; Chiriva-Internati, M.; Hegazi, M.A.A.A.; Bresalier, R.S.; Hassan, C.; Repici, A.; Carrara, S. Fractal nature of human gastrointestinal system: Exploring a new era. *World J. Gastroenterol.* **2023**, *29*, 4036–4052. [CrossRef] [PubMed]
30. Badea, A.F.; Lupsor Platon, M.; Crisan, M.; Cattani, C.; Badea, I.; Pierro, G.; Sannino, G.; Baciut, G. Fractal analysis of elastographic images for automatic detection of diffuse diseases of salivary glands: Preliminary results. *Comput. Math. Methods Med.* **2013**, *2013*, 47238. [CrossRef] [PubMed]
31. Horsburgh, A.; Massoud, T.F. The salivary ducts of Wharton and Stenson: Analysis of normal variant sialographic morphometry and a historical review. *Ann. Anat.* **2013**, *195*, 238–242. [CrossRef] [PubMed]
32. Rakonczay, Z., Jr.; Vág, J.; Földes, A.; Nagy, K.; Nagy, Á.; Hegyi, P.; Varga, G. Chronic inflammation in the pancreas and salivary glands–lessons from similarities and differences in pathophysiology and treatment modalities. *Curr. Pharm. Des.* **2014**, *20*, 1104–1120.
33. Makdissi, J.; Feinberg, L.; Roy, A. Is there a role for ultrasound-guided balloon sialoplasty technique in salivary gland structures? *Dentomaxillofac. Radiol.* **2017**, *46*, 20170088. [CrossRef] [PubMed]
34. Frulloni, L.; Morana, G.; Bovo, P.; Mansueto, G.C.; Vaona, B.; Di Francesco, V.; Procacci, C.; Cavallini, G. Salivary gland involvement in patients with chronic pancreatitis. *Pancreas* **1999**, *19*, 33–38. [CrossRef] [PubMed]
35. Varghese, J.C.; Thornton, F.; Lucey, B.C.; Walsh, M.; Farrell, M.A.; Lee, M.J. A prospective comparative study of MR sialography and conventional sialography of salivary duct disease. *AJR Am. J. Roentgenol.* **1999**, *17*, 1497–1503. [CrossRef] [PubMed]
36. Harrison, J.D. Re: Magnetic resonance identification of an accessory submandibular duct and gland: An unusual variant. *J. Laryngol. Otol.* **2008**, *122*, 1015.
37. Nayak, S.B. Accessory submandibular salivary gland forming a "horseshoe" with the main submandibular salivary gland: A unique variation. *J. Craniofac. Surg.* **2018**, *29*, 1376–1377. [CrossRef]